

# Compact Radio Structure of the High-Redshift BL Lac Object 0820+225

Valeriu Tudose<sup>1,2</sup>, Denise C. Gabuzda<sup>3</sup>, Alina-Catalina Donea<sup>4,2</sup>

<sup>1</sup> “Anton Pannekoek” Astronomical Institute, University of Amsterdam, <sup>2</sup> Astronomical Institute of the Romanian Academy, <sup>3</sup> Department of Physics, University College Cork, <sup>4</sup> Centre for Stellar and Planetary Astrophysics, Monash University

## Abstract

We report the results of four-epoch multi-frequency radio monitoring of the distant ( $z = 0.95$ ) BL Lac object 0820+225. The observations were carried out between September 2000 and July 2002 at 5, 8 and 15 GHz with the Very Long Baseline Array. The total intensity and linear polarization maps exhibit remarkable stability over the time scale of these observations and are consistent with earlier multi-frequency VLBA observations of this source. The presence of differential Faraday rotation along the jet is confirmed; in particular, there is enhanced Faraday rotation near a sharp bend in the jet. The increased sensitivity and improved baseline covered of these new images has enabled us to detect two regions of emission at 15 GHz that were not evident in the earlier images, whose position is coincident with prominent jet components observed at the lower frequencies. The overall properties of the jet in the context of possible magnetic field geometries and the interaction of the jet with the surrounding medium are discussed.

## 1. Polarization Maps

Figures 1-3 present 5.0, 8.4 and 15.4 GHz total-intensity contours with superposed polarization electric-field vectors for two of our four epochs. The similarity of the total-intensity and polarization structures at the two different epochs is striking. The increased sensitivity and improved baseline coverage of these new maps has enabled us to detect at all four epochs two regions of emission at 15.4 GHz that were not evident in the earlier images (at coordinates [-10,-8] and [-16,-16] in Fig. 3), whose position is coincident with prominent jet emission observed at the lower frequencies (Gabuzda, Pushkarev & Garnich 2001). The radio emission of 0820+225 is dominated by processes taking place in optically thin emission regions in the jet, where the magnetic-field vectors are almost perpendicular to the electric-field vectors in the observer's frame (they are not exactly orthogonal due to the transformations between the reference frames). The degree of polarization in the jet (Fig. 4) is typically 5-15%, but reaches appreciably higher values along the northwestern edge and end of the jet. The overall stability of the total intensity and polarization structure over a period of some five years (1997—2003) is somewhat surprising and difficult to understand, particularly given various evidence suggesting that the jet may be actively interacting with its surrounding medium.

## 2. Spectral Index Distribution

The distribution of the spectral-index  $\alpha$  ( $F_\nu \sim \nu^\alpha$ ) in Fig. 5 was made using the data at 5.0 and 8.4 GHz from epoch C. The errors in the accompanying plots are statistical. The object is dominated by the contribution of optically thin emission regions in the extended jet. The characteristic jet spectral indices are  $\alpha \sim -1$  to  $-1.5$  (right two plots in Fig. 5), somewhat steeper than is typical. The spectrum in the most prominent knots flattens somewhat, but remains quite steep. As was pointed out by Gabuzda et al. (2001), the knot at position [-1,-8] in Fig. 5, which coincides with the first sharp apparent bend of the jet, exhibits an appreciably flatter spectrum than the rest of the jet, suggestive of low-frequency absorption and possibly an interaction site between the jet and external medium. The flattening of the spectrum in the knots further away from the core is more likely associated with acceleration processes that affect the hard tail of the electron distribution.

## 3. Rotation Measure Distribution

Rotation measure (RM) maps depict the distribution of the frequency dependence of the observed polarization position angles (PAs), assuming Faraday rotation to be at work along the line of sight towards the target. The Faraday rotation represents the rotation of the plane of polarization of a linearly polarized wave propagating through a magnetized plasma with a non-zero magnetic-field component along the line of sight. Its characteristic signature is a “ $\lambda^2$ ” variation of the PAs. Fig. 6 presents the RM map constructed with the three-frequency data from epoch A, after removing the constant Galactic RM contribution determined from integrated measurements at lower frequencies (Pushkarev 2001). The errors in the plots are statistical. The RM distribution is shown in two separate maps displaying two different RM ranges, which highlight the RM behavior in the inner (left) and outer (right) jets. The plots clearly display local Faraday rotation near the core region, confirming the results of Gabuzda et al. 2001. In particular, there is a marked enhancement of the Faraday rotation in the same region where the spectrum substantially flattens near the first sharp apparent bend in the jet. It is natural to interpret this in terms of an enhancement of the free-electron density in this region, consistent with the presence of free-free absorption there. A RM gradient from the inner jet toward the first bend is clearly visible. The right-hand RM map also suggests that enhanced Faraday rotation is at work along the line of sight toward the knot near coordinates [-16,-16] in Fig. 6, and there is evidence for an increase in the local rotation measure toward the end of the jet. Thus, relatively high RM values seem to be associated with the two brightest knots in the jet. The parsec-scale inhomogeneities in the observed RM distribution cannot be accounted for by plasma clouds in our own Galaxy. This means that the Faraday rotation must be produced in the immediate vicinity of the jet, so that the intrinsic RMs (i.e., in the comoving frame) will be a factor of  $(1+z)^2 \sim 4$  higher (to correct for the expansion of the Universe).

## 4. Magnetic Field Structure

Fig. 7 shows the orientation of the magnetic-field vectors in the observer's frame after the effect of the Faraday-rotation distribution is removed. The structure of the magnetic field is stable over the entire timescale covered by our observations (the map on the right is taken from Gabuzda et al. 2001). Near the core, the magnetic field is nearly perpendicular to the jet axis, a statistical tendency observed in BL Lac objects (Gabuzda et al. 1992; Marscher et al. 2002). This orientation is usually interpreted either as a sign of relativistic shocks that enhance the local magnetic field in the plane of compression (Laing 1980) or as a signature of an intrinsic magnetic field with a helical structure for which, in the comoving frame, the toroidal component is comparable to or stronger than the poloidal component (Gabuzda 1999; Meier, Koide & Uchida 2001; Lyutikov, Pariev & Gabuzda 2005). Further from the core (starting at coordinates around [-10,-7] in Fig. 7), the magnetic field begins to be aligned with the jet direction, remaining aligned as the jet bends. Given the curved appearance of the jet, this longitudinal magnetic field may be due to a shear interaction between the jet and external medium, as is suggested by the higher degree of polarization measured along the western edge of the jet (Fig. 4). However, a helical magnetic field will also display a longitudinal component offset toward the edge of the jet for some viewing angles, providing an alternative explanation for the appearance of this longitudinal field. The magnetic field again becomes closer to orthogonal to the jet direction further down the jet (at about coordinates [-17,-20] in Fig. 7), undergoing a jump by approximately 90 degrees. The origin of this rotation in the magnetic-field orientation is not clear.

## References

- Gabuzda, D.C., 1999, New Astron. Rev., 43, 691
- Gabuzda, D.C., Cawthorne, T.V., Roberts, D.H., Wardle J.F.C., 1992, ApJ, 388, 40
- Gabuzda, D.C., Pushkarev, A.B., Garnich, N.N., 2001, MNRAS, 327, 1
- Laing, R., 1980, MNRAS, 193, 439
- Lyutikov, M., Pariev, V.I., Gabuzda, D.C., 2005, MNRAS, 360, 869
- Marscher, A.P., Jorstad, S.G., Mattox, J.R., Wehrle, A.E., 2002, ApJ, 577, 85
- Meier, D.L., Koide, S., Uchida, Y., 2001, Science, 291, 84
- Pushkarev, A.B., 2001, Astron. Rep., 45, 667

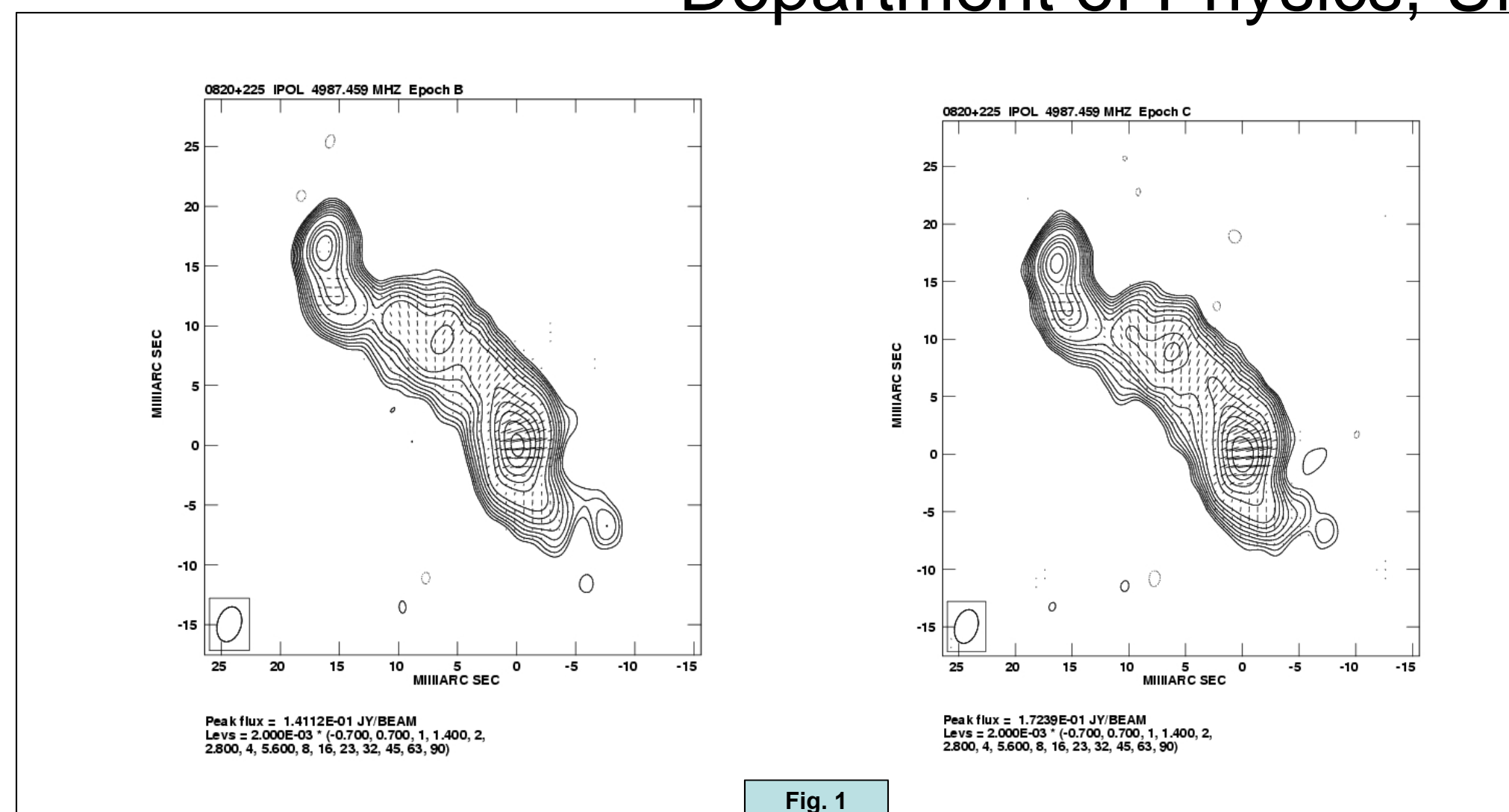
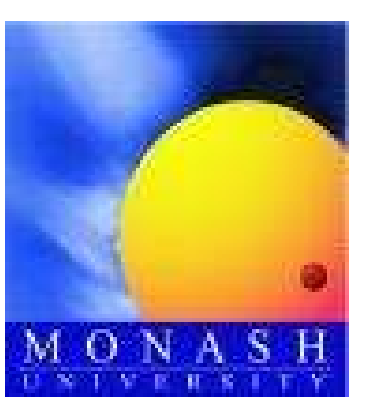


Fig. 1

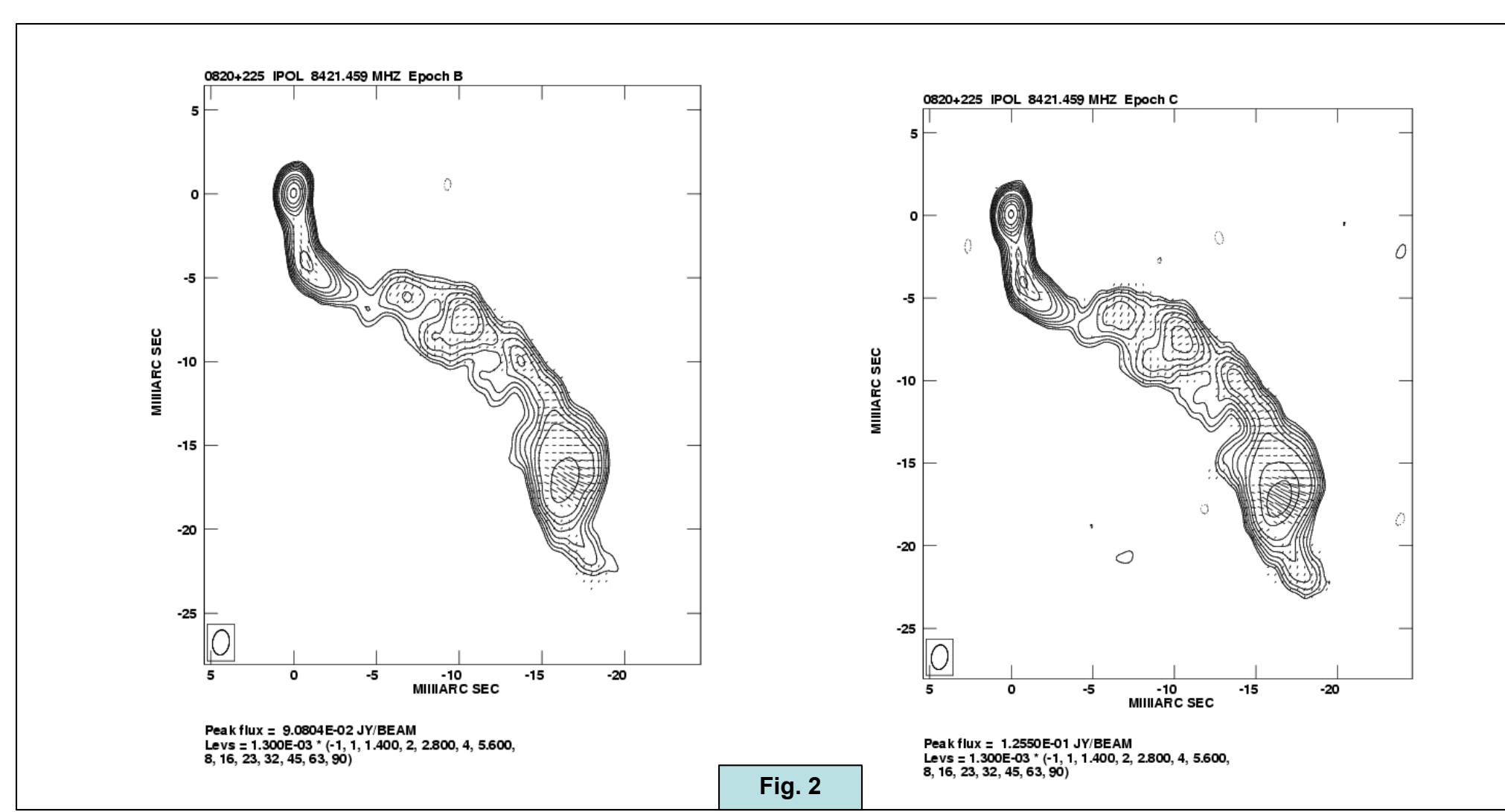


Fig. 2

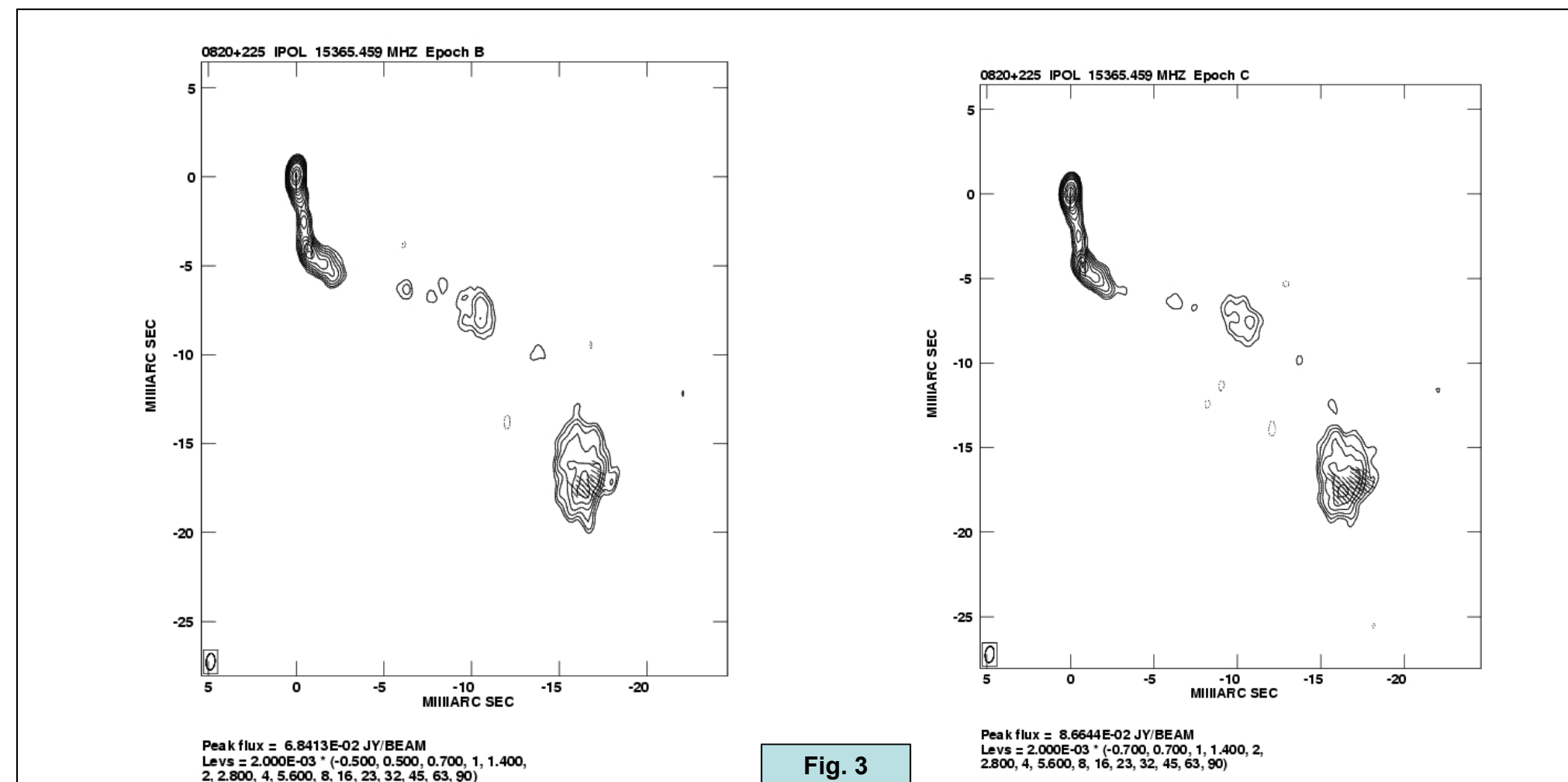


Fig. 3

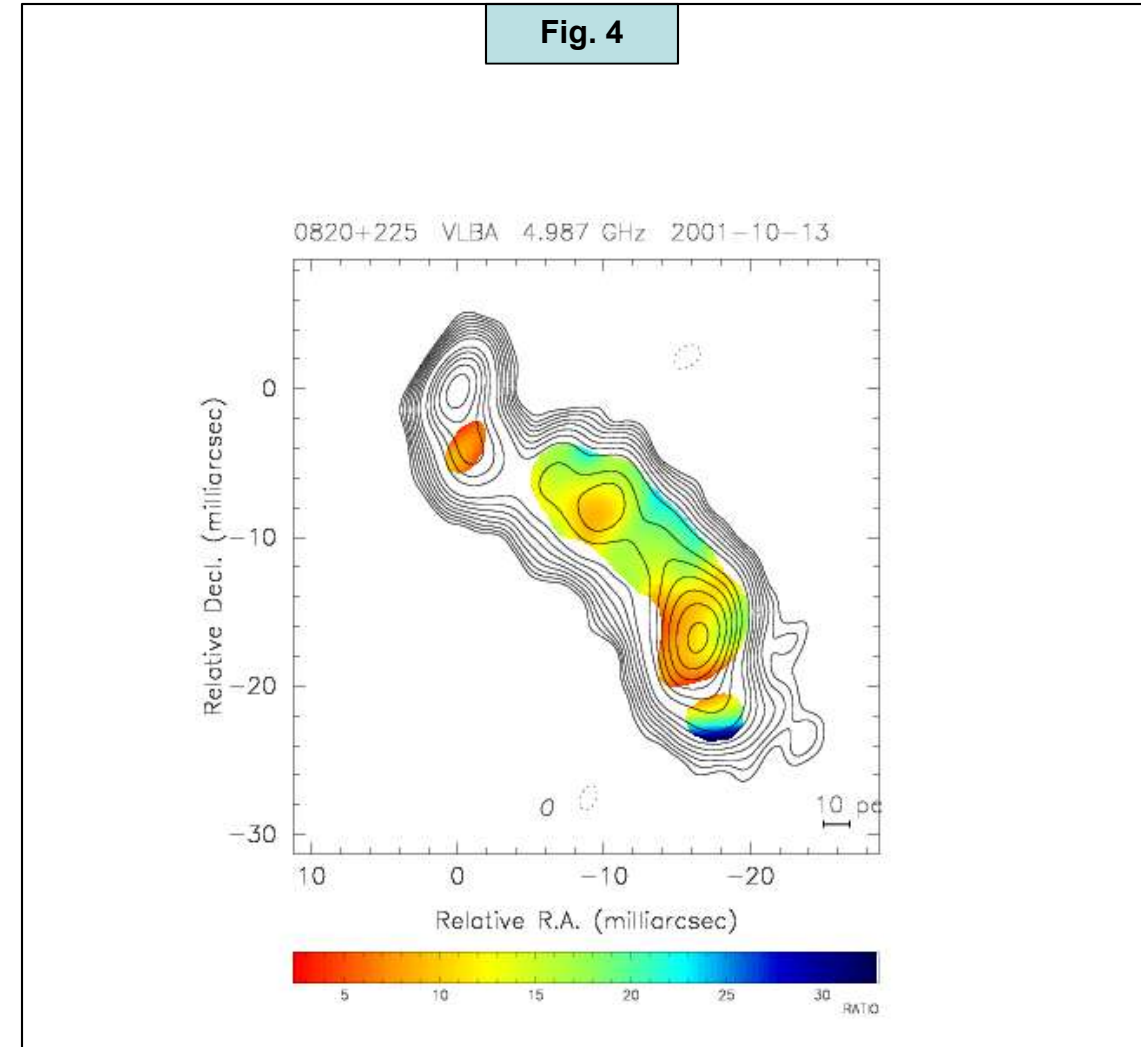


Fig. 4

Epoch	Date
A	September 24, 2000
B	May 11, 2001
C	October 13, 2001
D	July 17, 2002

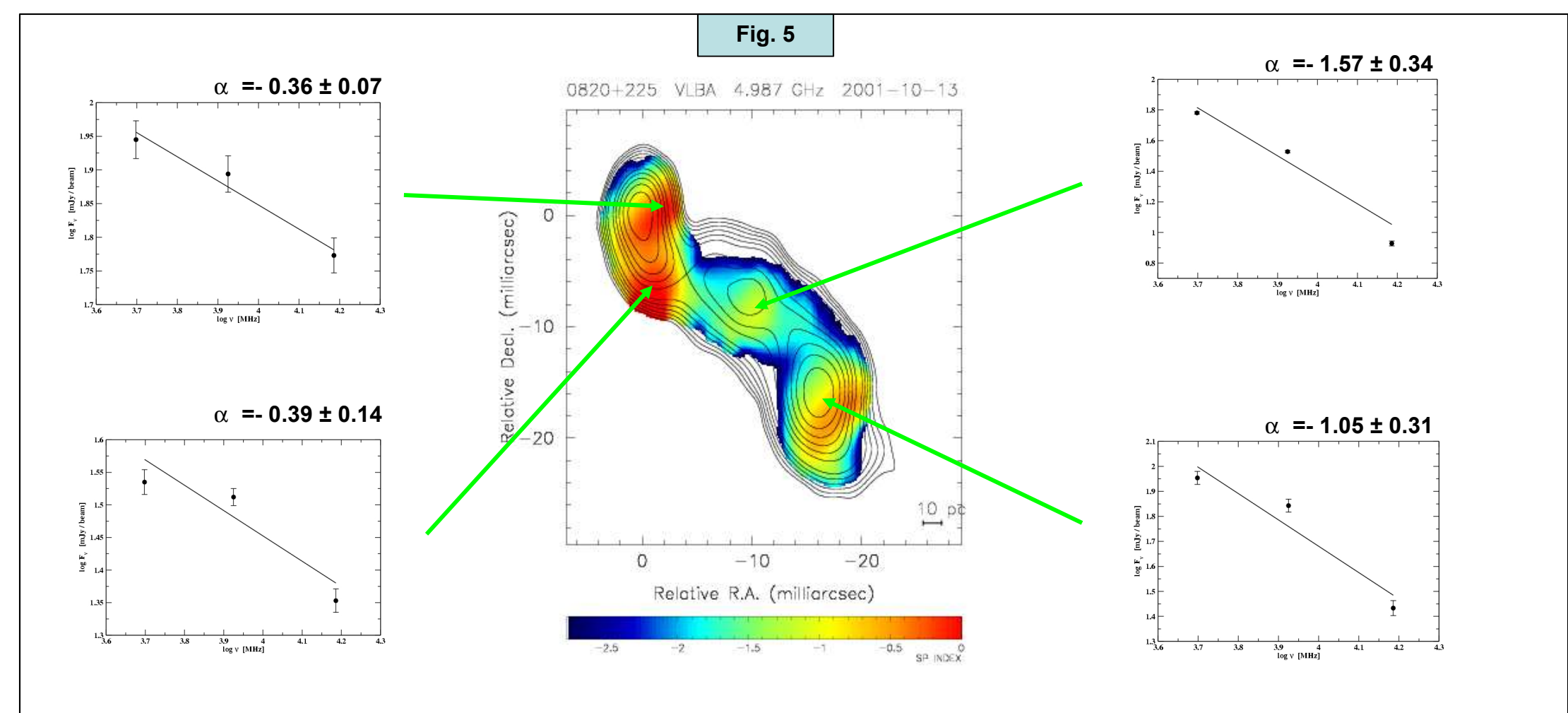


Fig. 5

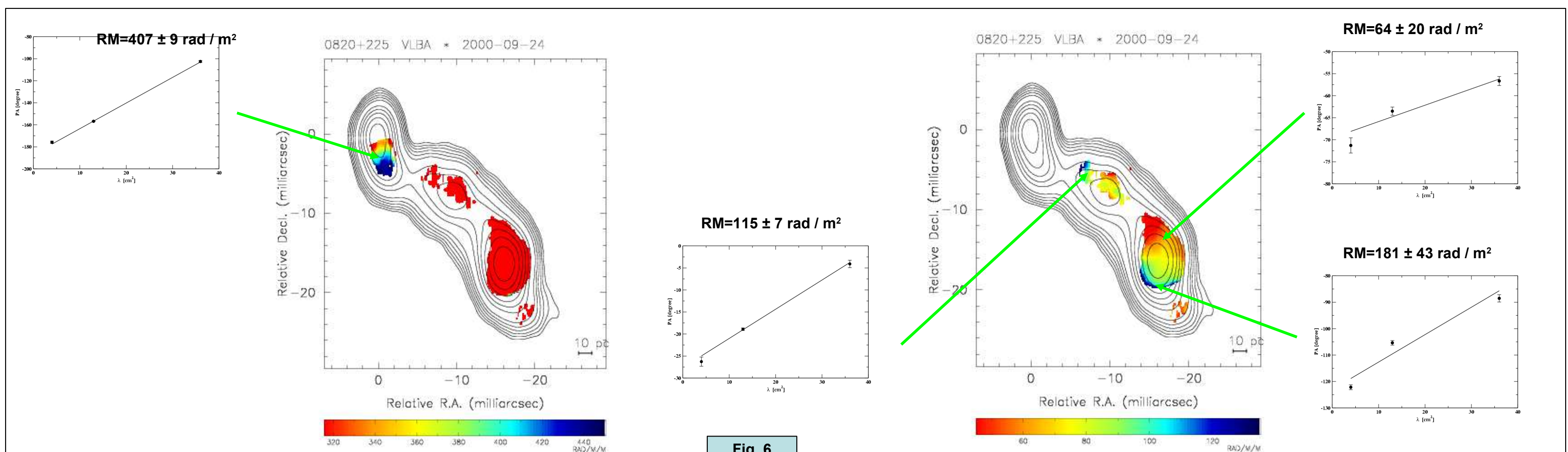


Fig. 6

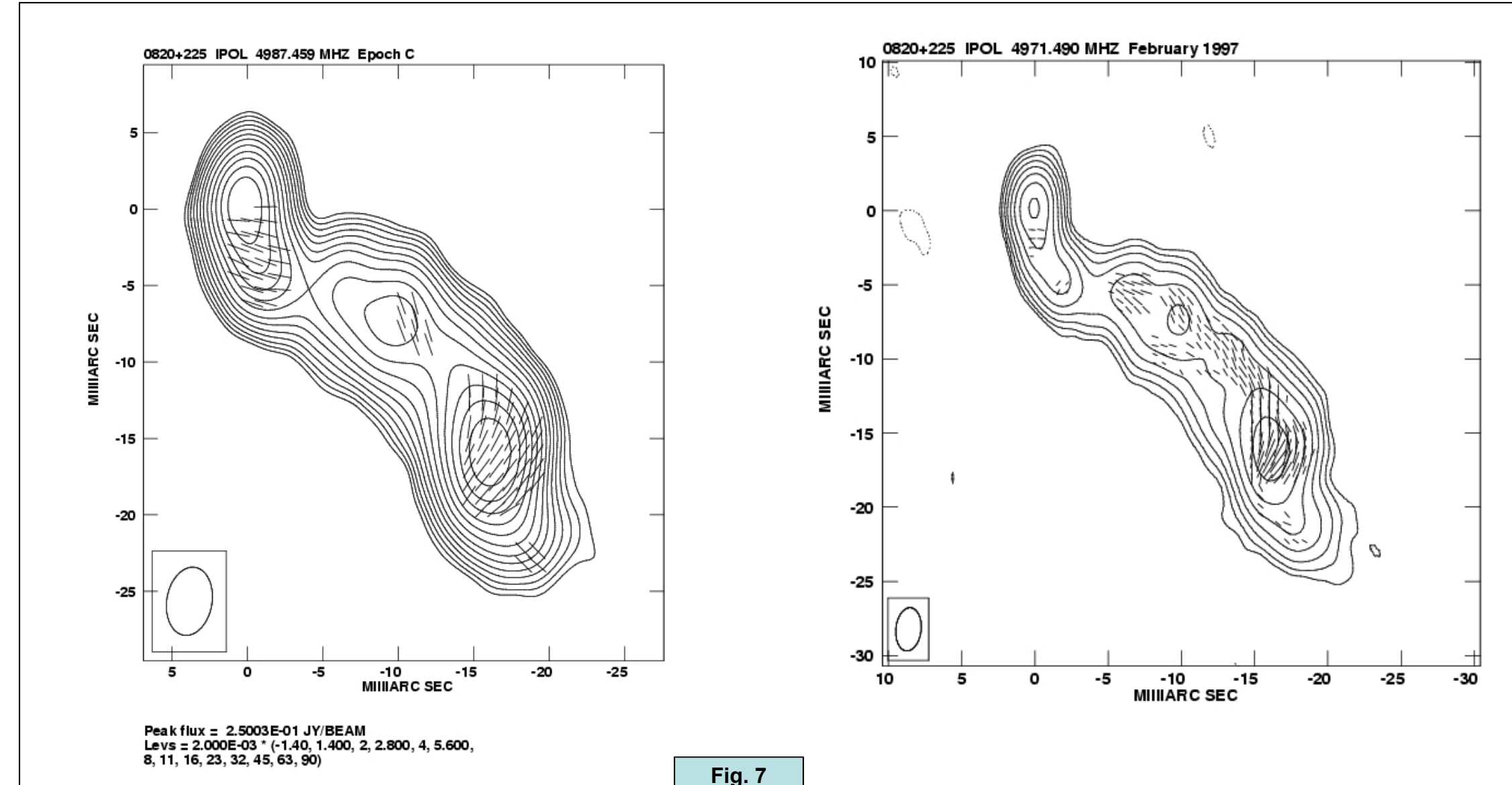


Fig. 7